

A COMPARISON BETWEEN DISTANCE PROTECTION AND DIFFERENTIAL PROTECTION WITHOUT SYNCHRONIZATION

Dipl.-Ing. Michael Albert
Saarland University
Saarbruecken, Germany

Univ.-Prof. Dr.-Ing. Hans-Jürgen Koglin
Saarland University
Saarbruecken, Germany

Dr.-Ing. Michael Igel
ALSTOM Energietechnik GmbH
Heiligenhaus, Germany

albert@lev.ee.uni-sb.de

koglin@lev.ee.uni-sb.de

michael.igel@tde.alstom.de

Abstract – Differential protection algorithms normally need synchronized sampled values at the terminals of a multi terminal line for comparison. Using the new differential protection algorithms it is possible to observe the protection zone without synchronized samples. These new algorithms use the positive sequence components of the currents and the voltages at the tap points. Then, using line parameters and the first Kirchhoff law, the protection zone is observed. Calculating the positive sequence components at each terminal, it is possible to economise the data rate and minimise the effort for calculating the sum at the tap point.

These methods were tested using a 110 kV multi terminal line. The next step in the processing is to expand the simulation and the investigation to other voltage levels. To that end the utilizability of the algorithms in medium voltage is investigated. These experiences can lead to an advanced adjustment of the tapping characteristic. Subsequently the results of the algorithms are compared with the results of a distance protection relay which is normally used to protect transmission lines. Finally the comparison between these two different methods is presented and the advantages and disadvantages of each protection method are shown.

Keywords: *Differential protection, digital algorithms, distance protection, symmetrical components, power transmission lines*

1 INTRODUCTION

One of the main difficulties in protection is to guarantee selectivity. For this, the use of differential protection is becoming more important. In contrast to distance protection it is able to realize a reliable fast time tripping of the protection zone. But it needs a great amount of data in comparison with distance protection for analyzing the protection zone. The measured currents and voltages

have to be transferred to the measurement points and above all they have to be sampled synchronously. This very aspect of synchronous sampling data means additional expenses with regard to the measurement equipment.

In a former paper [1] new methods of differential protection were presented which did not need synchronized sampling data. The currents and voltages were translated at the tap point. By calculating the admittances or the powers at the tap point the unknown phase shifts due to the not synchronized data were eliminated. Additionally it is possible to calculate the phase shift from the voltages in a prefault stage. These methods can be used to protect simple lines, multi-terminal lines and tapped lines.

In this paper these differential protection aspects are investigated for some special fault conditions and compared with distance protection. All the investigations given in chap. 3 and 4 were intensively investigated using the EMTP packet. In the paper the investigation results are presented. The results show that the differential protection algorithms presented in this paper are the best solution for protecting multi-terminal lines or tapped lines. The comparisons prove that the distance protection is too uncertain for a selective protection system.

2 BASICS

2.1 New differential protection algorithms

With eq. (1), voltage and current at the tap point can be calculated from voltage and current at the terminal using the line parameters. The equation for section A of the line shown in Fig. 1 is:

$$\begin{pmatrix} \underline{U}_{LA} \\ \underline{I}_{LA} \end{pmatrix} = \begin{pmatrix} 1 + j\omega \frac{C_A}{2}(R_A + jX_A) & -(R_A + jX_A) \\ \frac{\omega C_A^2}{4} \left(R_A + j \left(X_A - \frac{4}{\omega C_A} \right) \right) & 1 + j\omega \frac{C_A}{2}(R_A + jX_A) \end{pmatrix} \begin{pmatrix} \underline{U}_A \\ \underline{I}_A \end{pmatrix} \quad (1)$$

At the tap point the first Kirchhoff law yields

$$\underline{I}_{\perp A} + \underline{I}_{\perp B} + \underline{I}_{\perp C} = 0 \quad (2)$$

Here attention has to be paid to the not synchronized values. Since the currents at the tap point are calculated by eq. (1) for the sound line, there will be a discrepancy $\underline{\Delta I}_{\perp}$ in eq. (2) for the faulted line. Normally this discrepancy is related to the sum of the absolute values

$$|\underline{\Delta I}_{\perp}| = \frac{|\underline{I}_{\perp A} + \underline{I}_{\perp B} + \underline{I}_{\perp C}|}{|\underline{I}_{\perp A}| + |\underline{I}_{\perp B}| + |\underline{I}_{\perp C}|} \quad (3)$$

If this relative discrepancy exceeds a given limit e.g. 0.1 a short circuit in the protection zone is recognized.

$$\text{Fault condition: } |\underline{\Delta I}_{\perp}| > 0.1 \quad (4)$$

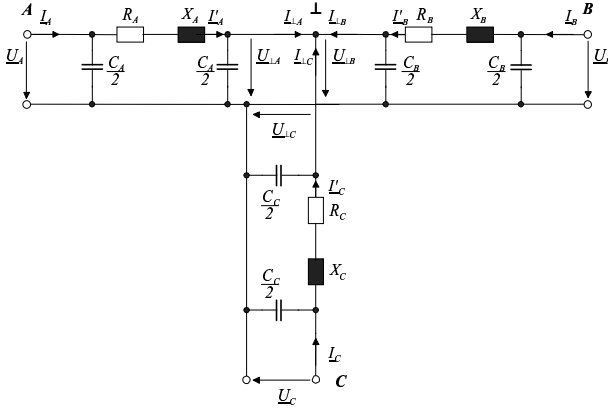


Figure 1: Equivalent scheme of a three-terminal line; \perp - tap point; A, B, C - measured terminals of the three line sections

2.1.1 Admittance and Power Approach

In the admittance approach the currents of eq. (2) are divided by the voltage at the tap point:

$$\underline{Y}_{\perp A} + \underline{Y}_{\perp B} + \underline{Y}_{\perp C} = \frac{\underline{I}_{\perp A}}{\underline{U}_{\perp A}} + \frac{\underline{I}_{\perp B}}{\underline{U}_{\perp B}} + \frac{\underline{I}_{\perp C}}{\underline{U}_{\perp C}} = 0 \quad (5)$$

In the case of fault the relative discrepancy of the sum of the admittances is

$$|\underline{\Delta Y}_{\perp}| = \frac{|\underline{Y}_{\perp A} + \underline{Y}_{\perp B} + \underline{Y}_{\perp C}|}{|\underline{Y}_{\perp A}| + |\underline{Y}_{\perp B}| + |\underline{Y}_{\perp C}|} \quad (6)$$

$$\text{and the fault condition } |\underline{\Delta Y}_{\perp}| > 0.1 \quad (7)$$

The admittances do not rely upon the synchronization.

In the power approach the conjugated currents of eq. (2) are multiplied by the voltage at the tap point:

$$\underline{S}_{\perp A} + \underline{S}_{\perp B} + \underline{S}_{\perp C} = \underline{U}_{\perp A} \underline{I}_{\perp A}^* + \underline{U}_{\perp B} \underline{I}_{\perp B}^* + \underline{U}_{\perp C} \underline{I}_{\perp C}^* = 0 \quad (8)$$

In the case of a fault the relative discrepancy of the sum of the apparent power is

$$|\underline{\Delta S}_{\perp}| = \frac{|\underline{S}_{\perp A} + \underline{S}_{\perp B} + \underline{S}_{\perp C}|}{|\underline{S}_{\perp A}| + |\underline{S}_{\perp B}| + |\underline{S}_{\perp C}|} \quad (9)$$

$$\text{and the fault condition } |\underline{\Delta S}_{\perp}| > 0.1 \quad (10)$$

The apparent power does not rely upon the synchronization. The apparent power eq. (9) can be divided into one equation for the active power and one for reactive power

$$P_{\perp A} + P_{\perp B} + P_{\perp C} = 0 \quad (11)$$

$$Q_{\perp A} + Q_{\perp B} + Q_{\perp C} = 0 \quad (12)$$

In a case of fault the relative discrepancies for active and reactive power are

$$|\underline{\Delta P}_{\perp}| = \frac{|\underline{P}_{\perp A} + \underline{P}_{\perp B} + \underline{P}_{\perp C}|}{|\underline{P}_{\perp A}| + |\underline{P}_{\perp B}| + |\underline{P}_{\perp C}|} \quad (13)$$

$$|\underline{\Delta Q}_{\perp}| = \frac{|\underline{Q}_{\perp A} + \underline{Q}_{\perp B} + \underline{Q}_{\perp C}|}{|\underline{Q}_{\perp A}| + |\underline{Q}_{\perp B}| + |\underline{Q}_{\perp C}|} \quad (14)$$

$$\text{Fault conditions: } |\underline{\Delta P}_{\perp}| > 0.1 \quad (15)$$

$$|\underline{\Delta Q}_{\perp}| > 0.1 \quad (16)$$

2.1.2 Current Approach or Synchronization by Measurements

In the current approach the currents of eq. (2) are synchronized by

$$\underline{U}_{\perp A} = \underline{U}_{\perp B} = \underline{U}_{\perp C} = \underline{U}_{\perp} \quad (17)$$

calculated by eq. (1) using the measurements at the terminals of the line. This simple and low cost method to synchronize the phasors consists in finding the desynchronization angles in the pre-fault stage. In the case of fault on the line these angles are kept constant.

The complex domains in which the phasors of the currents and voltages of the different line terminals are represented (characterized by $^{(A),(B)}$ or $^{(C)}$) are not synchronized. The complex domains are so defined, that the voltages of the line terminals in the pre-fault stage are purely real:

$$\underline{U}_A^{(A)} = U_A ; \underline{U}_B^{(B)} = U_B ; \underline{U}_C^{(C)} = U_C \quad (18)$$

Then the currents can be expressed by their active and reactive part:

$$\underline{I}_A^{(A)} = I_{wA} - jI_{bA} ; \underline{I}_B^{(B)} = I_{wB} - jI_{bB} ; \underline{I}_C^{(C)} = I_{wC} - jI_{bC} \quad (19)$$

To process these quantities together they are transformed in a common complex domain which is so defined, that the phasor of the voltage at the tap point in the pre-fault stage is purely real

$\underline{U}_{\perp} = U_{\perp} \cdot 1$. Therefore the complex domains of the different line terminals are shifted by the line angle ϑ . The complex quantities of this common complex domain are not especially characterized. For section A of Fig. 1 the voltage at the tap point has to be calculated by eq. (1) as a synchronizing equation:

$$\underline{U}_{\perp A} = U_{\perp A} = (1 + j\omega \frac{C_A}{2} (R_A + jX_A)) U_A e^{-j\vartheta_A} + (R_A + jX_A)(I_{wA} - jI_{bA}) e^{-j\vartheta_A} \quad (20)$$

$$\underline{U}_{\perp A} = U_{\perp A} = (E_{\perp A} + jF_{\perp A}) e^{-j\vartheta_A} \quad (21)$$

where

$$E_{\perp A} = (1 - \omega \frac{C_A}{2} X_A) U_A - R_A I_{wA} - X_A I_{bA} \quad (22)$$

$$F_{\perp A} = \omega \frac{C_A}{2} R_A U_A - X_A I_{wA} + R_A I_{bA} \quad (23)$$

Then

$$U_{\perp A} = \sqrt{E_{\perp A}^2 + F_{\perp A}^2} \quad (24)$$

and

$$\vartheta_A = \arctan\left(\frac{F_{\perp A}}{E_{\perp A}}\right) \quad (25)$$

The synchronizing equations for the other line terminals can be derived similarly.

These synchronizations are executed in pre-fault stage which is defined by eq. (17) and

$$|\underline{U}_{\perp}| > 0.8 \frac{U_n}{\sqrt{3}} \quad (26)$$

In the case of a fault the currents $\underline{I}_{\perp A}^{(A)}$; $\underline{I}_{\perp B}^{(B)}$; $\underline{I}_{\perp C}^{(C)}$ at the tap point are calculated by eq. (1) using the measured quantities $\underline{U}_A^{(A)}$; $\underline{U}_B^{(B)}$; $\underline{U}_C^{(C)}$ and $\underline{I}_A^{(A)}$; $\underline{I}_B^{(B)}$; $\underline{I}_C^{(C)}$.² The currents at the tap point are then transformed into the common complex domain using eq. (19)

$$\underline{I}_{\perp A} = \underline{I}_{\perp A}^{(A)} e^{-j\vartheta_A}; \underline{I}_{\perp B} = \underline{I}_{\perp B}^{(B)} e^{-j\vartheta_B}; \underline{I}_{\perp C} = \underline{I}_{\perp C}^{(C)} e^{-j\vartheta_C} \quad (27)$$

In the case of fault the relative discrepancy of the sum of the currents is

$$|\underline{\Delta I}_{\perp r}| = \frac{|\underline{I}_{\perp A} + \underline{I}_{\perp B} + \underline{I}_{\perp C}|}{|\underline{I}_{\perp A}| + |\underline{I}_{\perp B}| + |\underline{I}_{\perp C}|} \quad (28)$$

and the fault condition $|\underline{\Delta I}_{\perp r}| > 0.1$ (29)

¹ The common complex domain can be any other e.g. the complex domain of one of the line terminals.

² Note: In case of fault the voltages of the line terminals are not real anymore in their complex domains, because of the sudden phase shift due to the short circuit. And the real and imaginary parts of the currents are not anymore the active and reactive components.

2.2 Distance Protection

Distance protection relays have been used for years to protect lines. For this comparison a digital distance protection algorithm is used. There are a lot of different methods for calculating the impedances from the sampling data. The algorithm applied in this paper uses a first order line model to calculate the impedance. Using 4 sampling values the real and the imaginary part of the impedances are:

$$R = \frac{u_2(i_4 - i_2) - u_3(i_3 - i_1)}{i_2(i_4 - i_2) - i_3(i_3 - i_1)} \quad (30)$$

$$X = 2 \sin \Delta \cdot \frac{(u_3 i_2 - u_2 i_3)}{i_2(i_4 - i_2) - i_3(i_3 - i_1)} \quad (31)$$

$$\text{with } \Delta = \omega \cdot \Delta t \quad (32)$$

and Δt is an equidistant time step [2].

3 SIMULATION AND FAULT CONDITIONS

3.1 General Information

All the investigations were made using the EMTP packet. Fig. 3 shows the ATP model used for simulation. The nominal voltage of the simulated network is normally 20 kV, except for the simulations of the saturation effects. These simulations were made for a nominal voltage of 110 kV. The sampling rate in all investigations is 1 kHz. The simulation time and the time of the fault occurrence are varied. The lines are simulated using the distributed line model. The investigations were carried out for different tap points, different fault locations, fault resistances and kinds of faults.

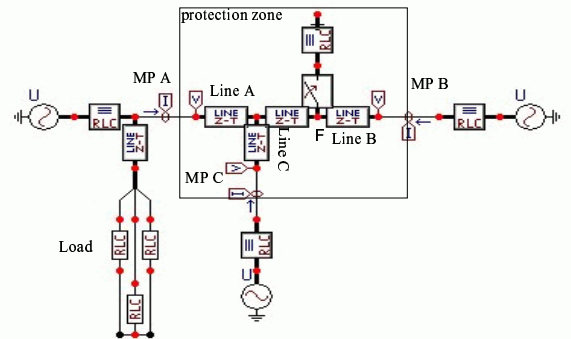


Figure 2: ATP/EMTP-Simulated three-terminal line 22kV

For each fault, the relative discrepancies (6), (13), (14) and (28) were calculated. The impedances (30) and (31) were also estimated.

3.2 Special Fault Conditions

Additionally to these standard cases some investigations were made for special fault conditions. In regard of these special fault conditions a discrimination is necessary between multi-terminal lines, lines having three or more terminals with substantial generation behind each, and tapped lines, lines having one or more terminals with substantial generation behind them and taps feeding load only. These taps do not have sufficient current feed-back to operate relays [5].

Under these circumstances for example external faults, saturation effects of the current transformer and outfeed conditions are investigated.

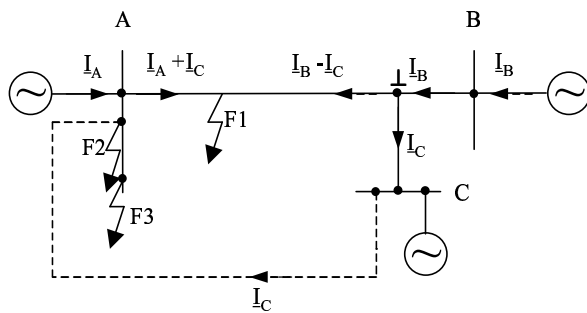


Figure 3: Outfeed condition

Fig. 3 shows the situation of the outfeed condition. This may occur in the case of a weak terminal C, interconnected externally to terminal A. The short-circuit current can flow out of terminal C and contribute to the short-circuit current of terminal A. Under these circumstances directional or phase comparison relays at terminal C may fail to operate because the fault is seen in the reverse direction [5].

4 RESULTS

In a former paper [1] the results for single phase and three phase faults under normal condition were presented. For this case the following tables and figures contain the results of special fault conditions (chap. 3) in regard of the results of the distance protection algorithm.

4.1 Outfeed condition

Fig. 3 shows the three different faults simulated for the outfeed condition. The fault F1 is a internal fault (2 km on line A), F2 is a internal fault near the busbar A and F3 is an external busbar fault at busbar A. All faults are three phase faults. The fault resistance for this investigations is $R_f=1 \Omega$.

In Fig. 4 the results of the current approach (28) are presented. A relative discrepancy near 1 means

there is a fault in the protection zone, a relative discrepancy near zero describes a faultless line. These investigations point out that this protection method can precisely discriminate external (F3) and internal faults (F1, F2).

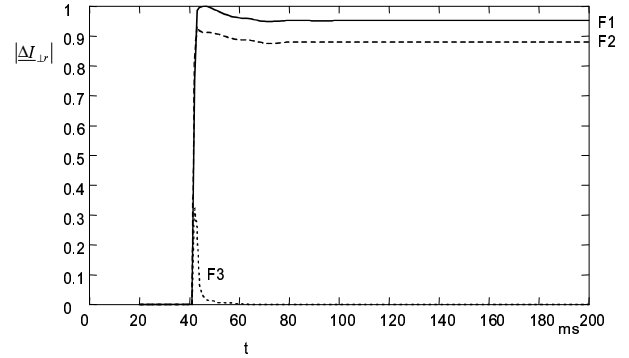


Figure 4: Current Approach (28) under different outfeed conditions (Fig. 3)

It is remarkable that for these cases the tripping time is very short, about <20 ms.

Fault	MP A	MP B	MP C
Faultless	R=1130 Ω X=-339 Ω	R=-441 Ω X=-16.4 Ω	R=679 Ω X=-116 Ω
F 1	R=1.6 Ω X=0.7 Ω	R=14.9 Ω X=6.5 Ω	R=-37.0 Ω X=36.5 Ω
F 2	R=1.1 Ω X=0.02 Ω	R=13.4 Ω X=3.7 Ω	R=-14.9 Ω X=5.9 Ω
F 3	R=-18.4 Ω X=7.3 Ω	R=13.4 Ω X=3.7 Ω	R=-14.9 Ω X=5.9 Ω

Table 1: Distance protection under different outfeed conditions (Fig. 3); MP: measuring point

The circumstances of the outfeed conditions cause problems using the distance protection algorithm.

Table 1 shows the investigation results of the distance protection algorithm. The impedances of the three measuring points are shown. The measuring point A can detect all three faults. The problems appear at the terminals B and C. At the measuring point B there is no possibility to differentiate between the internal fault F2 and the external fault F3 at the busbar A. More interesting is the behavior at the terminal C. For faultless condition the currents flow into the line. For the three faults from Fig. 2 the short-circuit current flow out of terminal C. A directional or phase comparison relay fail to operate because the fault is seen in the reverse direction.

The tripping time is difficult to estimate for these cases. The relays A and B will trip first. Then the short-circuit current at C will reverse and the relay C can trip.

4.2 Current transformer saturation

The current transformer saturation effects were simulated on three terminal-110 kV-line [1]. The current transformer on line A has saturation effects. Fig. 5 shows the current of one phase of a three-phase fault without resistance with saturation effects and the current of the same phase without saturation.

In Fig. 6 the current (28) and the active power approach (13) is shown. The fault location is on line A 10 km distant from the tap point. The relative discrepancy of the current approach points out that there is only a small gap using ideal measured values or using the values regarding the saturation effects. For the power and the admittance approach there are some problems with three-phase faults without fault resistance [1]. Further, Fig. 6 shows that the results even get better in the case of current transformer saturation.

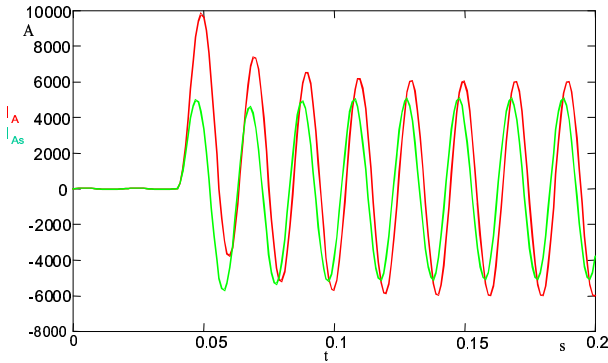


Figure 5: Current of phase A in case of a three phase fault with (I_{As}) and without (I_A) saturation effects

This effect is also recognizable in Fig. 7. Here the fault resistance is 1Ω . The current and the admittance approach are shown. For the results of the admittance approach the current transformer saturation has positive effects, too.

Thus it can be stated that saturation effects from one current transformer on internal faults have only small negative effects (current approach) and even positive effects on the power and admittance approaches.

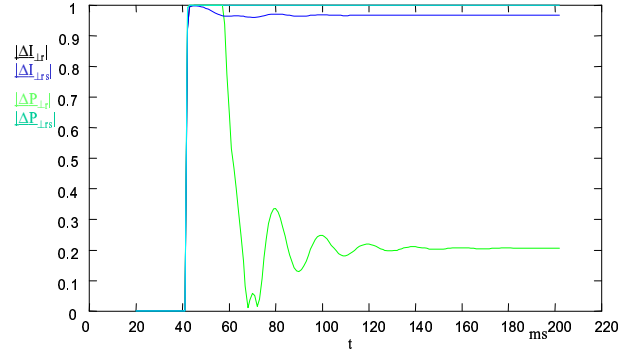


Figure 6: Current and active power approach with (ΔI_{lr_s} , ΔP_{lr_s}) and without (ΔI_{lr} , ΔP_{lr}) CT saturation, $R_f=0 \Omega$

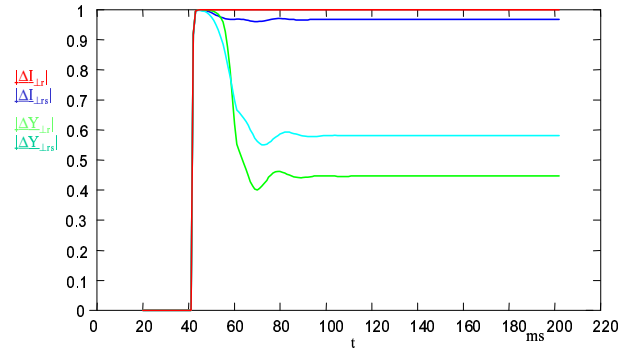


Figure 7: Current and admittance approach with (ΔI_{lr_s} , ΔY_{lr_s}) and without (ΔI_{lr} , ΔY_{lr}) CT saturation; $R_f=1 \Omega$

4.3 Fault with small fault currents

The influence of the fault resistance on the results of the current approach is shown in Fig. 8. The simulation of three different loads is taken into account. The loads $P=0$ MW, 4.38MW and 30MW were connected at busbar B.

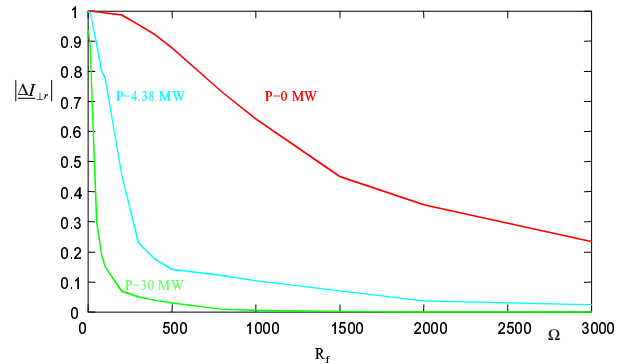


Figure 8: Current approach (28) for a single phase fault, different fault resistances and different loads

The fault resistance varies from 0Ω up to $3 \text{ k}\Omega$. Fig. 8 spots that the bigger the load on the line, the less the fault resistance that can be detected in the case of single phase faults. But up to a resistance of 100Ω there is no problem recognizing the faults. With higher impedances and higher loads the relative discrepancy becomes less than 0.2.

The single-phase-to-earth faults carry out the main difficulties of distance protection. The distance zone reach problem is strongly dependent on the fault resistances. In Table 2 the impedances (30) and (31) are shown. For higher fault resistances the impedances of the faulty line are high. This means that in some cases a faultless line has a impedance in the same range.

	MP A	MP B	MP C
Fault-less	R=-3874 Ω X=-3858 Ω	R=1480 Ω X=-2236 Ω	R=2206 Ω X=-4922 Ω
R _f =0 Ω	R=5.3 Ω X=12.4 Ω	R=7.2 Ω X=15.9 Ω	R=4.7 Ω X=11.2 Ω
R _f =100 Ω	R=306.6 Ω X=1.8 Ω	R=343.2 Ω X=-28.9 Ω	R=273.1 Ω X=2.79 Ω
R _f =1k Ω	R=3441 Ω X=-2027 Ω	R=1458 Ω X=-957 Ω	R=2556 Ω X=-1361 Ω
R _f =3k Ω	R=-854 Ω X=-7673 Ω	R= 1598 Ω X=-1681 Ω	R=1674 Ω X=-5466 Ω

Table 2: Distance protection results for the faulty phase and different fault resistances

4.4 General comparison between distance and differential protection

Generally it can be stated that the distance protection needs a lot of adjustments for every line configuration. The protection relays have to be matched for every fault conditions and all kind of faults. That means a great amount of simulation and analyzing work. For the differential protection algorithms there is no need to adjust. The knowledge of line length, the topology of the protection zone and voltage level is sufficient for a satisfactory investigation.

The disadvantage of the differential protection is the need for communication between the measuring points and the data which have to be transmitted to all stations. But these new algorithms have the advantage that they need less data than the other differential protection methods. The current approach needs three real values at one sample, the admittance approach two real values and in terms of data rate the best methods are active and reactive power approaches. They need only one real value at one sample.

5 CONCLUSIONS

In the paper, the new differential protection algorithms of multi-terminal lines are proposed. The

algorithms do not require sampled values and therefore no synchronization. Four different criteria have been developed and investigated: admittance, active and reactive power and the current criteria.

The differential protection algorithms are tested under special fault conditions. The results are compared with the results of a distance protection algorithm. The outfeed condition, saturation effects and faults with small short-circuit currents are investigated. The differential protection methods can detect all faults. The internal and external faults are detected and the selectivity is guaranteed. The distance protection has problems detecting these kinds of faults. Internal faults with current transformer saturation effects and faults with small short-circuit currents can also be detected.

The disadvantage of differential protection, the great amount of data transfer between the measuring points, becomes less using these new algorithms. They need less data than traditional differential protection methods. A distance protection relay without telecommunications does not work accurately and it does not have the selectivity of these differential protection methods.

REFERENCES

- [1] H.-J. Koglin, M. Albert, M. Igel, T. Lobos and Z. Waclawek, "Differential Protection of Multi-Terminal Lines without Synchronization", PES IEEE Summer Meeting 2001.
- [2] G. Hosemann, T. Lobos, "Ermittlung der symmetrischen Komponenten durch Abtastalgorithmen", Archiv für Elektrotechnik 68 (1985) 1-16
- [3] H.-J. Koglin, T. Lobos, "Distanzschutz mit Mikrorechnern", etzArchiv Bd. 3 (1981) H.6
- [4] R. Speh, "Digitaler Netzschutz in Mittelspannungsnetzen", Dissertation, TH Darmstadt, 1985
- [5] CIGRE, "Application Guide on Protection of Complex Transmission Network Configurations", CIGRE SC34-WG04, May 1991
- [6] N. Schuster, "Schutz von Mehrendenleitungen im Hochspannungsnetz", Elektrizitätswirtschaft, vol. 99, 2000, pp. 12-17